Dynamics of Xe Atoms in NaA Zeolites and the 129Xe Chemical Shift

ARTICLE *in* CHEMINFORM · MARCH 1995

Impact Factor: 0.74 · DOI: 10.1021/j100009a003

2 AUTHORS:

Feng-Yin Li
National Chung Hsing University
57 PUBLICATIONS **825** CITATIONS
SEE PROFILE

Richard Stephen Berry
University of Chicago
513 PUBLICATIONS **15,420** CITATIONS
SEE PROFILE

Dynamics of Xe Atoms in NaA Zeolites and the ^{129}Xe Chemical Shift

Feng-Yin Li and R. Stephen Berry*

Department of Chemistry and The James Franck Institute, The University of Chicago, Chicago, Illinois 60637

Received: July 28, 1994; In Final Form: October 7, 1994[⊗]

Classical mechanical isothermal molecular dynamics simulations are used to model Xe atoms and Xe_N clusters trapped in the intracrystalline cavities of zeolite NaA, which is represented as a single α cage. An adsorption site model provides a means to investigate the nature of Xe atom adsorption, the site occupancy, and the rate of site-to-site exchange. Chemical shifts are computed for ^{129}Xe in the cavities, for single Xe atoms through clusters of Xe_9, from 150 to 420 K. An explanation is proposed for the large increase with N in the chemical shift from Xe_6 to Xe_7.

1. Introduction

Understanding the dynamical behavior of adsorbents in microporous solids is important in the use of molecular sieves for adsorption, catalysis, and chromatography. Due to the combination of their inertness and environmental sensitivity of their NMR spectra, ^{129}Xe atoms serve as good probes to investigate the properties of molecular sieves. Recently, the dynamics of rare gas atoms inside zeolite cavities has attracted attention.[1−6] Adsorbates larger than a certain size may be confined within a single cavity because of the atomic dimensions of the cavities and the narrow tunnels connecting these cavities. Experiments[1,2] indicate that the finite volume occupied by the Xe atoms trapped inside a single cavity becomes significant at high loading, which means Xe clusters may be formed under these conditions. If the influence of the Xe atoms in adjacent cavities is negligible, the dynamics of the Xe clusters inside zeolite cavities can be studied by extending the methods used for rare gas clusters in free space,[7−9] which have been well developed and can be easily adapted to study these systems. An important characteristic of clusters is the multiplicity of locally stable structures they exhibit or, in words aptly borrowed from hydrology, the multiplicity of "catchment basins" that occur on their potential energy surfaces. Each of these regions has an associated minimum-energy configuration for the cluster. With a little modification, our approach to this study is to investigate the relation between the thermodynamic and dynamical properties of occluded clusters in terms of the adsorption site of a single Xe cluster inside the α cavity.

Here, we use Nosé isothermal molecular dynamics simulations[10] to study the dynamics of different numbers of Xe atoms inside a single NaA zeolite α cavity at various temperatures. The purpose of this study is to report how the sodium cations, primarily the so-called type III Na^+ ions, and the Xe−Xe interactions influence aspects of Xe adsorption, particularly the site occupancy, the site-to-site exchange rate, and the way the number of Xe atoms inside the α cavity influences the ^{129}Xe chemical shifts. The essence of this study is the division of the cavity into several sites according to the potential of interaction of these sites with a single Xe atom inside the cavity and then the analysis of the dynamics of occupancy of the sites by Xe atoms. In section 2, we describe the model representing the clusters and the zeolite cavities and the methods used in this study. In section 3 we explain the results. With these findings, we try to understand the experimental ^{129}Xe NMR spectra of zeolite NaA, namely, the Xe chemical shifts and their dependence on cluster size and temperature. In particular, we examine the large increments of the Xe chemical shifts between Xe_6 and Xe_7, and between Xe_7 and Xe_8, which are almost twice those between cluster sizes smaller than Xe_6.[2] In section 4, we draw a conclusion from our results.

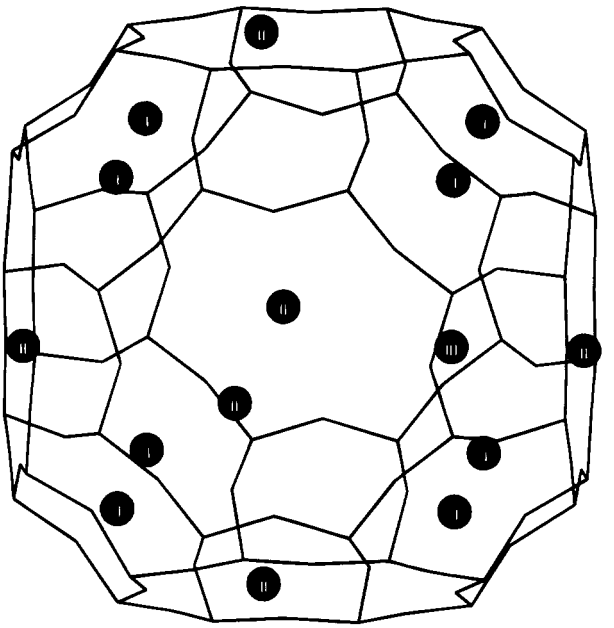

Figure 1. NaA zeolite α cavity. The vertices are positions of aluminum ions, and oxygen ions are approximately at the center of every edge. The black circles represent the sodium ions, and the number inside each circle indicates the type of sodium ion. The type III sodium ion is on the *XY* plane.

TABLE 1: Parameters Used in Calculation[a]

atom	r_{VDW}	$q/10^{-10}$ esu	C_l/kJ Å^6 mol^{-1}	B_l/kJ Å^{12} mol^{-1}
O	1.52	−0.7004	1.209×10^4	1.620×10^7
Na	1.17	+3.362	4.170×10^3	1.016×10^7

atom	σ/Å	ε/k	A/[stat−volt/cm]$^{-2}$	B/[stat−volt/cm]$^{-2}$
Xe	4.1	221	337.3	5396.8

[a] The parameters for sodium and oxygen are taken from ref 12, and the parameter A is taken from ref 14.

2. Model and Method

The potential function of the system is composed of two parts, atom−atom and atom−cavity interactions. We use a pairwise

[⊗] Abstract published in *Advance ACS Abstracts,* February 1, 1995.

0022-3654/95/2099-2459$09.00/0

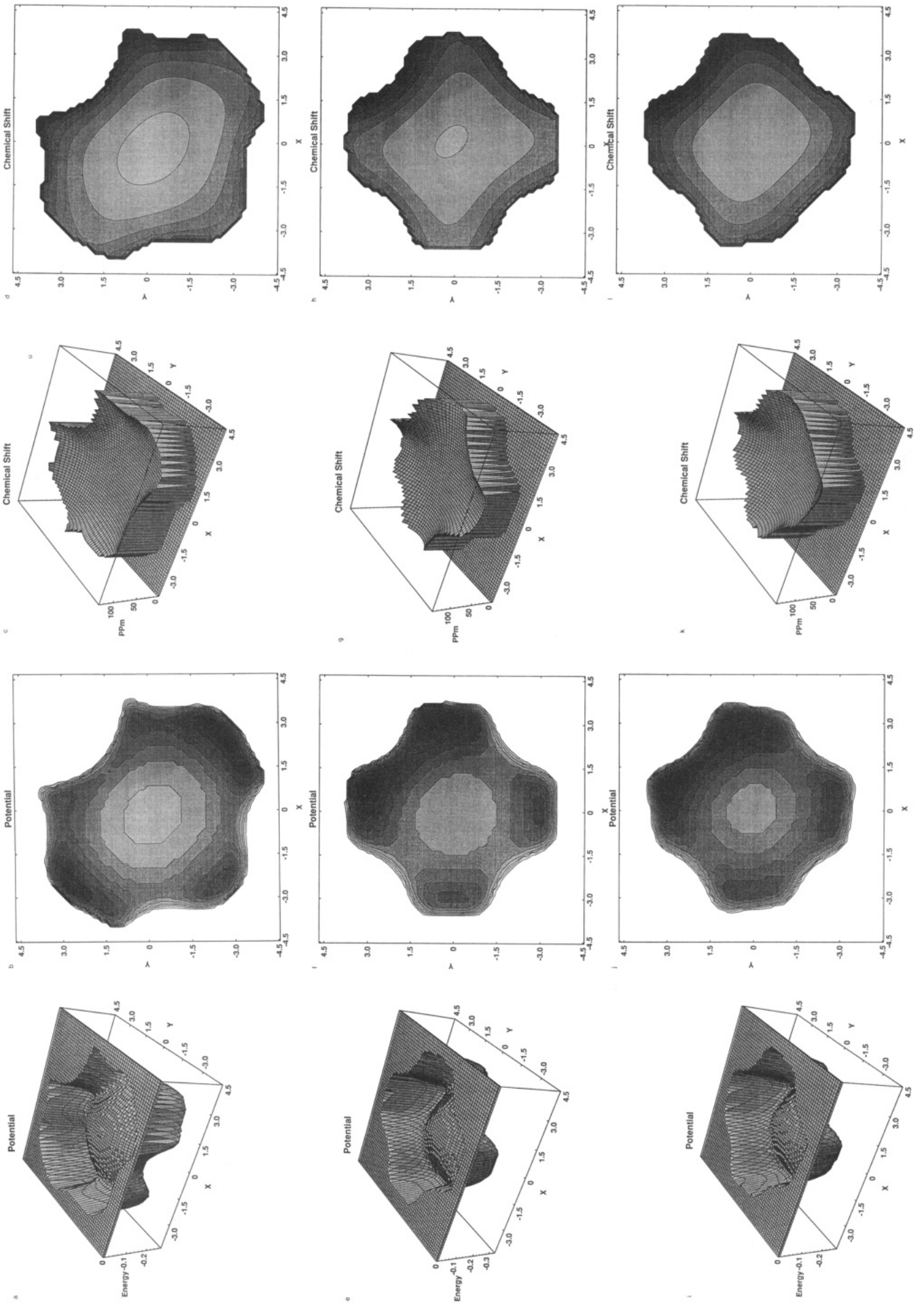

Figure 2.

Lennard-Jones 6-12 potential to describe the atom−atom interactions. To facilitate the calculation, a model zeolite cavity is represented as a rigid structure containing 72 oxygen ions and 15 sodium ions. The positions of the framework atoms are taken from literature.[11] The model cavity is shown in Figure 1. The Xe−framework interaction includes repulsion, dispersion, and induced dipole−static electric field interactions. The form of interaction, charges, atomic sizes, and both repulsive and dispersion constants are taken from van Tassel, *et al.*[12] Our cavity corresponds to their cation-saturated single-cage system. The constants we use are shown in Table 1.

Isothermal molecular dynamics trajectories are generated by using Nosé's method with the first-order, six-value form of Gear's method[13] as the propagator. The integration time step, Δt, is 5×10^{-15} s, and the length of a typical trajectory is 10 ns. The initial configuration is generated by running isoenergetic molecular dynamics and perodically using a steepest descent quench to obtain the structures corresponding to the local minima. These are verified from the eigenvalues of the Hessian matrix at the minimum. The locally stable configuration with the lowest energy is selected as a starting point. It is then randomly twisted and equilibrated to the desired temperature with isothermal molecular dynamics.

The ^{129}Xe chemical shift in NaA zeolite has been calculated recently by Jameson *et al.*[6] Here we use a simple approximate method to investigate the chemical shift change with different numbers of Xe atoms in a NaA zeolite cavity. The estimated chemical shift δ is calculated from the following equation:

$$\delta = \frac{A}{N}\sum_{k=1}^{N}\langle\epsilon^2\rangle + \frac{B}{N}\sum_{i=1}^{N}\sum_{i\neq j}^{N}\langle\overline{F^2}\rangle \qquad (1)$$

where N is the number of Xe atoms inside the cavity, ϵ is the electric field due to the sodium and oxygen ions, $\overline{F^2}$ is the mean square effective field created at one Xe atom due to the dispersion interaction between it and the other Xe atoms inside the cavity. The angular brackets denote an average over the entire trajectory. The coefficient A is taken from literature,[14] and B is calculated by fitting the results of a calculation for Xe_2 at a temperature above 300 K to the experimental result of Jameson *et al.*[2] In the simple London approximation, the mean square field at atom 1 due to atom 2 can be calculated as

$$\overline{F^2} = \frac{3}{2}\alpha_2(0)\frac{U_1U_2}{U_1+U_2}R^{-6} \qquad (2)$$

where U_1 and U_2 are the ionization potentials of atoms 1 and 2, both of which are Xe atoms here, $\alpha_2(0)$ is the static polarizability, and R is the distance between atoms 1 and 2.

3. Results and Discussion

A. Adsorption Sites of a Single Xe Atom. We use a single Xe atom as a test particle moving inside the cavity to examine the contour of the Xe−cavity potential and the chemical shift. Figure 2 shows the potential energy and chemical shift in a plane containing the type III sodium ion and in the planes above and below. The position dependencies of both the potential energy and the chemical shift show extrema due to the sodium ion which occupies the center of one of the four-membered rings. But how does this sodium ion influence the adsorption dynamics? First, we must identify the adsorption sites, *i.e.*, the locations corresponding to energy minima of a single Xe atom inside the cavity. We begin with a classical molecular dynamics simulation. Then, by periodically quenching the kinetic energy of the Xe atom and applying the method of steepest descent to its representative point in phase space, we presumably find the stationary point at the bottom of the catchment basin closest to where the atom was when the quench was applied. We then check whether the stationary point is truly a minimum by finding the eigenvalues of the Hessian matrix at that point. With this method, we have been able to find 13 different minima for a xenon atom in an α cavity. These locations as well as the corresponding potential energies and chemical shifts are shown in Figures 3, 4, and 5, respectively. There is a locally stable site for the Xe atom in each eight-membered ring and four-

Figure 2. Potential and chemical shift of a single Xe atom inside the cavity. The figures in the top row are constructed for $Z = 0.0$ Å, *i.e.*, the XY plane containing the type III sodium ion. The middle row is in the plane at $Z = 2.0$ Å, and the bottom row is in the plane at $Z = -2.0$ Å. The unit of potential energy is 10^5 J/mol, and the unit for chemical shift is ppm. The units of X and Y are both angstroms. Parts a, e, and i are the three-dimensional plots of potential energy; parts b, f, and j are the corresponding contour plots; parts c, g, and k are the corresponding three-dimensional plots of chemical shift, and parts d, h, and l are the corresponding contour plots.

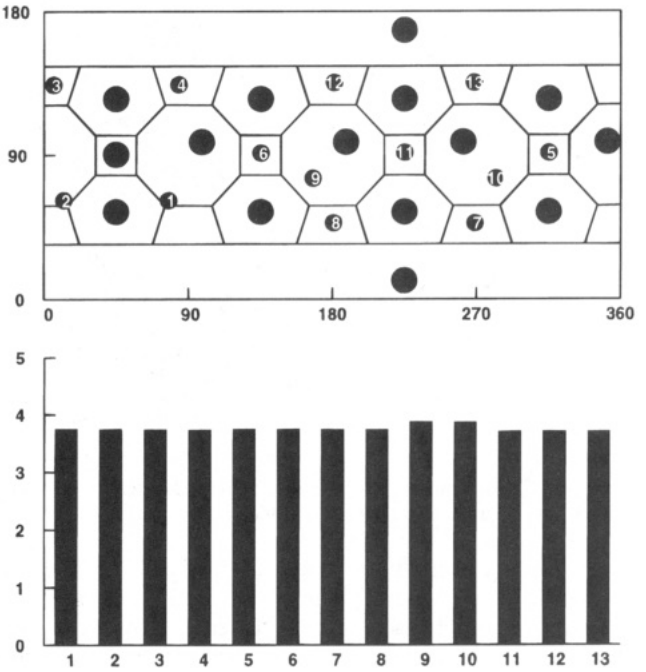

Figure 3. Locations of the adsorption sites for a single Xe atom inside the cavity. The upper graph is the angular part of the spherical coordinate; the lower graph is the radial part. The large black circles are the positions of sodium ions. The numbers in the small black circles indicate the sequence of the adsorption sites from lowest energy site to highest energy site. The unit of length on the Y axis of the lower graph is angstroms.

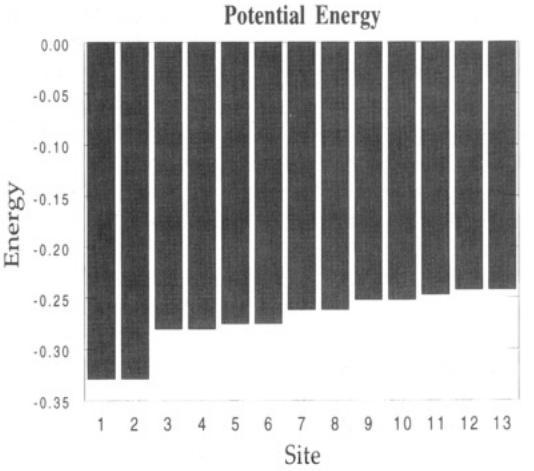

Figure 4. Potential energies of the adsorption sites. The unit of energy is 10^5 J/mol. The order of the sites is the same as in Figure 3.

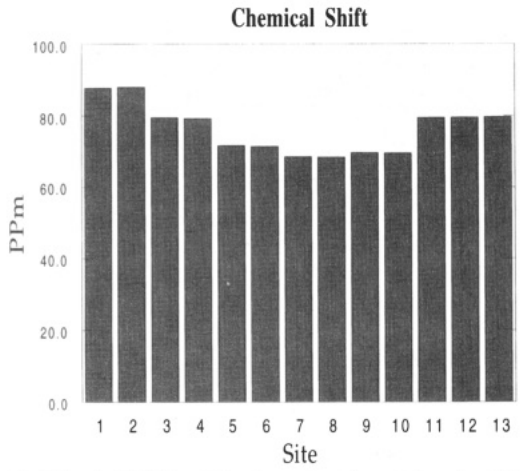

Figure 5. Chemical shifts of the adsorption sites. The unit of chemical shift is ppm. The order of the sites is the same as in Figure 3.

membered ring, except those containing the type III sodium ion. It is not surprising that the two strongest adsorption sites are on both sides of this sodium ion in the eight-membered rings.

The distances between sites 8 and 9 and between sites 7 and 10 are only 1.97 Å. If sites 8 and 9 are counted as only one site, and likewise sites 7 and 10, then the effective number of sites is 11, the number of minima found by Jameson *et al.*[6] However the differences we found between the energies of the minima are much larger than those reported by Jameson.[6]

B. Adsorption Sites of Larger Xe Clusters. By using the same method, the minimum-energy structures of the larger Xe clusters can be found. Figure 6 shows the structures of Xe_5, Xe_6, and Xe_7. They have particularly long durations, compared with other structures. It is worth noting that the Xe atoms of these systems are all adsorbed within 1 Å of the adsorption sites found in the previous section. Instead of occupying the sites with low adsorption energy, such as site 4, the Xe atoms of the minimum structures of Xe_5 and Xe_6 occupied high adsorption energy sites. This indicates that Xe−Xe repulsion plays a very important role in the well residence time, since the distance between sites 3 and 4 is 3.37 Å. It is the minimum-energy structures of Xe_7 with longer well residence times that begin to occupy site 4, the available site of lowest energy. This means that the largest Xe cluster that can be found inside the cavity without large Xe−Xe repulsion is Xe_6.

C. Comparison with a Homogeneous Cavity. The minimum-energy structures of the Xe cluster inside the structured cavity we have been discussing are quite different from the structures inside a homogeneous continuous cavity of similar dimensions. To make this comparison, we modeled the Xe−cavity interaction as a Morse potential with the same isothermal MD algorithm. We averaged the Xe−cavity potential energy of the structured cavity over all of the inner surface and then fitted the parameters of a uniform Morse potential (normal to the cavity surface, of course) to match that averaged Xe−cavity interaction potential. The minimum-energy structures of Xe clusters inside the homogeneous, continuous cavity show no preferential adsorption sites and aggregate together to form a quasi-two-dimensional adsorbed layer, like a film, if the Xe cluster contains fewer than seven atoms. A transition occurs from a quasi-two-dimensional adsorption to a two-layer adsorption when the number of Xe atoms goes from 6 to 7. This phenomenon is never observed in the structured cavity model when the number of Xe atoms is less than 9. By varying the Xe−wall interaction, we find that Xe−Xe interaction plays an important role in both the surface and the two-layer adsorption. At high temperature, Xe atoms in quasi-two-dimensional

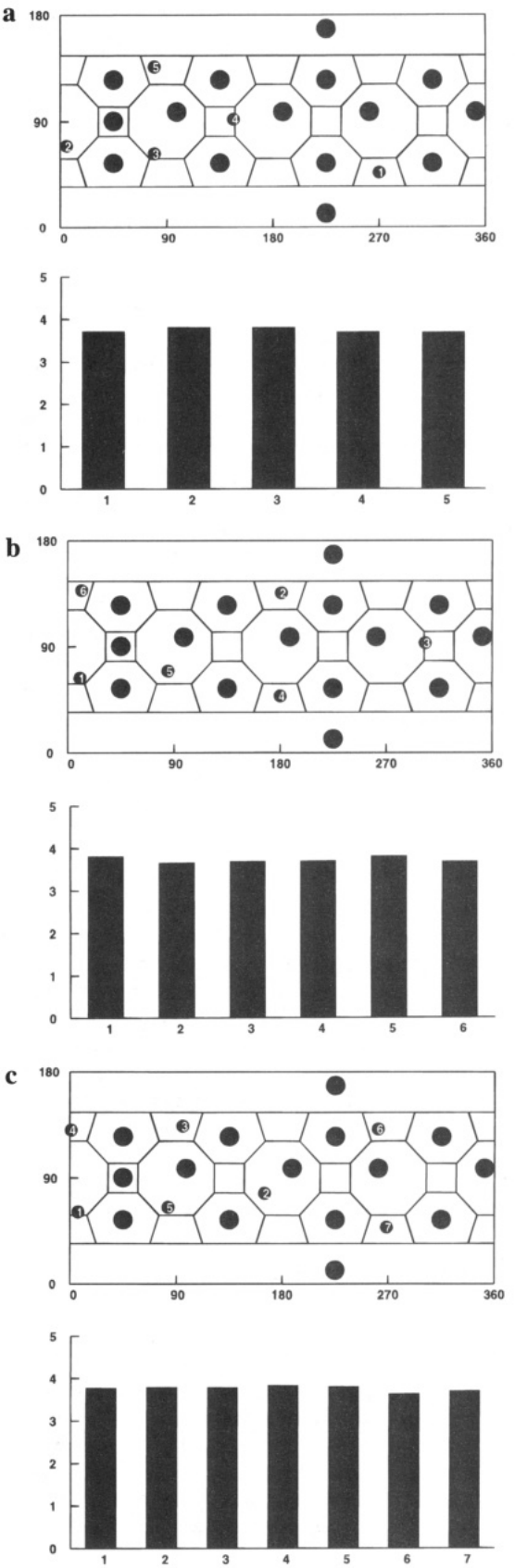

Figure 6. Minimum-energy structures of Xe_5, Xe_6, and Xe_7 with long durations. The format is similar to Figure 3 except that the numbers in the small black circles are just labels of the Xe atoms. All the axes and units are the same as in Figure 3. Part a is Xe_5; part b is Xe_6; part c is Xe_7.

adsorption behave like a two-dimensional liquid. Since we modeled the cavity as a spherical cage, the tangential motion of Xe atoms on the inner surface of the cavity is influenced

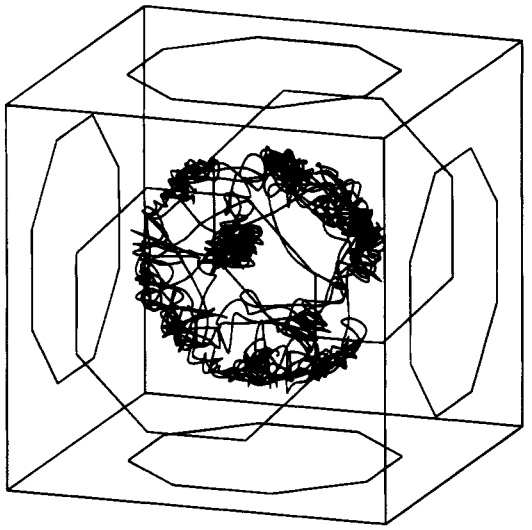

Figure 7. Three-dimensional plot of a 50-ps trajectory of Xe_6. The octagon in each face of the cubic represents the eight-membered ring. The black lines are the trajectories of each Xe atom. The vertices of each octagon are positions of the aluminum ions.

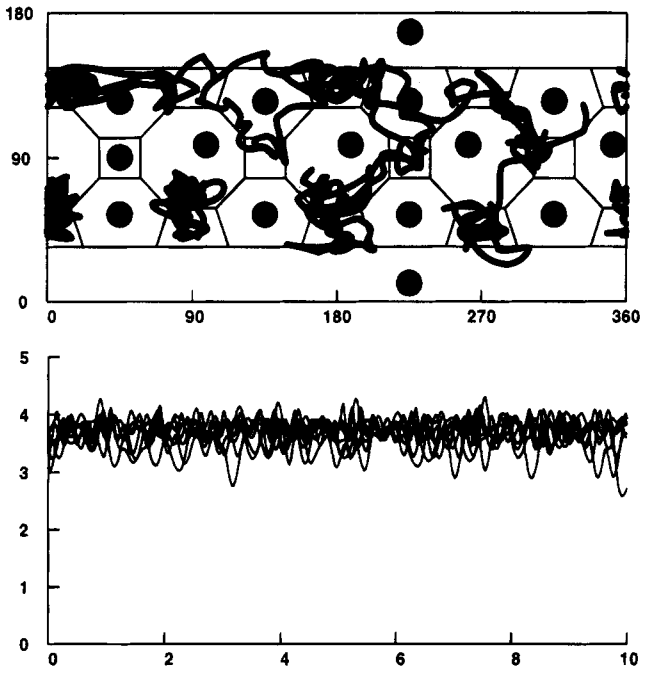

Figure 8. 25-ps interval of the previous trajectory. The upper graph is the angular part, similar to Figure 3. The lower graph is the radial part. The unit of the *Y* axis is angstroms; the unit of the *X* axis is 2.5 ps.

only by Xe−Xe interaction. The collisions between Xe atoms cause a transfer from radial motion to tangential motion and thus make the quasi-two-dimensional layer behave like a film. In the larger Xe_N clusters, $N > 7$, there are enough Xe atoms on the cavity surface to force new atoms to form the second layer, whose precise structure is due to the Xe−Xe interations. In this study of the simple homogeneous cavity, we find that although the Xe−Xe interaction is much weaker than the Xe−wall interaction, it still plays a key factor in controlling the dynamics of the Xe adsorption in the cavity. Now the question is what role the Xe−Xe interaction plays in the atomic network cavity.

D. Dynamics of Site-to-Site Exchange. To analyze the dynamics of the site-to-site exchange, we define an Xe atom as adsorbed whenever it is closer than 1.68 Å to a particular site. We choose this value to maximize the areas of the adsorption sites and at the same time still distinguish among the different adsorption sites, except for sites 6, 8, 9 and sites 5, 7, 10, which we consider to behave as single sites due to their proximity and similarity. With this definition, we are able to study the nature of the adsorption and the site-to-site exchange rate and will describe them now. Figure 7 shows a 50-ps trajectory of an occluded Xe_6 cluster at 300 K. To visualize the dynamics of site-to-site exchange, we plot this trajectory in spherical coordinates. A 25-ps section of trajectory is shown in Figure 8. This is presented in two graphs respectively showing the evolution of the (polar) angular and radial spherical coordinates. It is clear that in this trajectory Xe atoms are trapped at sites 1 and 2, but travel among the other sites due to the large differences in the energies of the adsorption sites and of the barriers that separate them.

To analyze the nature of the adsorption sites, let us return to the case of a single Xe atom. We consider three diagnostic properties that we have extracted from statistical analyses of the constant-temperature dynamics of site-to-site movement. These are the fraction of time spent in each kind of site, which we call the "relative site-occupancy time"; the percentage of desorptions from a site that are followed by immediate return and readsorption to that site or one of the same kind; and the average residence or dwell time in each site. Tables 2, 3, and 4 show some statistics of each of these three measures of site-to-site exchange of Xe_1 at temperatures from 210 to 420 K. It is clear that sites 1 and 2 are the strongest adsorbing sites, exhibiting higher relative site-occupancy times and longer site-residence times, and have higher desorption-and-readsorption rates. As the temperature increases, the site-occupancy times, the adsorption-and-readsorption rates, and the site-residence times for sites 1 and 2 decrease, while those for the other sites gradually increase. The change in the relative site-residence times for sites 1 and 2 from 210 to 240 K (first two lines of Table 2) is a consequence of any real entropy differences between sites 1 and 2. At temperatures of 300 K and above, the strongly binding sites 1 and 2 lose much of their special character, according to the relative site-occupancy times and the return frequencies. The Xe atom naturally spends more time in desorbed status at higher temperatures, but the duration of times spent "in limbo" (column 0 of Table 2) and not at any specific site does not change very much with increasing temperature. This means the frequency of Xe atom desorption from adsorption sites increases along with temperature. When the temperature is higher than 300 K, the dynamics of the site-to-site exchange changes from mainly hopping between sites 1 and 2 to visiting the other sites more frequently, and the sum of the site-residence time of sites 1 and 2 becomes less than 50% of the whole trajectory.

By using the same method, we analyzed the systems from Xe_2 to Xe_7 inside the cavity. As shown in Table 5, the Xe atoms spend at least 83% of the time during a 1-ns trajectory in these 13 adsorption sites. This indicates the system is much like a two-dimensional, adsorbed system, except that the surface has negative curvature, instead of being flat. It is clear that the relative site-occupancy times and the site-residence times of sites 1 and 2 decrease with increasing temperature, as they do for the single atom. However, these indices for "site" (5, 7, 10) and "site" (6, 8, 9) show rather complicated behavior with increasing temperature and the number of Xe atoms, reflecting an intricate balance between energy and entropy. The data of Tables 6 and 7 suggest that the Xe atoms experience difficulty in moving out of site 1 or 2, especially when the number of Xe atoms is as large as 7. This may due to the crowding of the Xe atoms inside the cavity. Even though the other sites show the same trend toward immobility as the number of Xe atoms in

TABLE 2: Percentages of Time Spent by a Single Atom in Each of the Nine Sites and Site Groups of the Structured Cavity, Which We Abbreviate as the "Relative Site-Occupancy Time" at Temperatures from 210 to 420 K, during a 1-ns Segment of a Trajectory[a]

	site									
temp	0	1	2	3	4	5, 7, 10	6, 8, 9	11	12	13
210	5.1	26.4	45.6	2.4	2.8	5.3	8.8	0.9	1.3	0.9
240	8.6	45.3	36.2	0.7	0.8	5.9	1.8	0.1	0.2	0.0
270	11.9	40.6	22.7	0.7	1.8	7.5	11.1	1.0	0.9	1.3
300	11.3	16.5	21.0	15.3	10.9	5.7	15.1	1.8	1.5	0.3
330	14.3	18.2	25.0	3.7	4.7	20.7	6.3	2.0	1.2	3.6
360	15.0	18.3	17.3	7.3	7.1	11.0	16.4	1.1	1.7	1.2
390	17.4	24.9	21.7	5.4	6.1	5.5	14.5	1.0	1.7	1.2
420	19.2	14.8	15.4	10.4	7.3	14.6	9.4	2.2	3.0	3.3

[a] The column labeled site 0 is the percentage of time that the Xe atom is not adsorbed to any site.

TABLE 3: Percentage of Desorption-and-Readsorption Events That Return a Single Xe Atom to the Same Site in the Cavity during a 1-ns Trajectory[a]

	site									
temp	0	1	2	3	4	5, 7, 10	6, 8, 9	11	12	13
210	53	81	77	0	0	28	33	0	20	0
240	44	75	73	0	0	50	50	0	0	0
270	45	69	53	0	0	0	10	0	0	0
300	32	56	59	20	11	28	22	0	0	0
330	30	45	50	8	25	13	11	0	0	0
360	23	42	42	9	16	11	9	0	10	10
390	35	46	50	31	19	8	16	33	0	14
420	22	28	37	30	15	11	18	0	8	7

[a] Here, the column labeled site 0 is the average percentage of all events. The group of sites 5, 7, and 10 are treated as one site, as is the group consisting of sites 6, 8, and 9.

TABLE 4: Average Residence Time per Visit for a Single Xe Atom in the Cavity during a 1-ns Trajectory[a]

	site									
temp	0	1	2	3	4	5, 7, 10	6, 8, 9	11	12	13
210	0.6	12.6	17.5	6.1	4.8	2.5	4.9	4.7	2.6	8.9
240	0.9	12.2	9.8	7.3	8.1	3.2	3.0	1.9	2.0	0.6
270	1.0	7.6	7.1	3.9	6.2	3.5	3.7	3.5	1.9	2.6
300	0.7	6.6	6.5	5.3	4.0	1.3	5.6	4.6	1.9	2.6
330	0.8	4.5	5.2	3.1	3.9	3.0	2.3	3.3	3.0	4.6
360	0.8	4.8	4.5	3.5	3.9	2.1	2.4	1.4	2.9	3.2
390	0.8	4.1	4.1	2.9	2.9	3.2	2.7	1.7	2.5	1.8
420	0.7	3.3	3.2	2.6	2.2	1.8	1.9	1.8	2.5	2.4

[a] The unit is picoseconds. The column labeled site 0 is the average dwell or residence time for the Xe atom, between hopping events that take it from site to site. The group of sites 5, 7, and 10 are again treated as one site but normalized, i.e., divided by 3; the same is true for sites 6, 8, and 9.

the cavity increases, the Xe atoms can move among these sites more easily than between sites 1 and 2. We can therefore conclude that there are two kinds of motion in the site-to-site exchange dynamics. Some of the Xe atoms march on low ground within the zones of sites 1 and 2, while the others move readily from site to site among the other seven sites and site groups. Once in a while, a Xe atom adsorbed in site 1 or 2 pops out of that site and joins the fast motion, and soon thereafter, one of the fast moving Xe atoms drops into the newly formed vacancy site in the lower level. Effective site (5, 7, 10) and effective site (6, 8, 9) act like busy traffic intersections and allow the Xe atoms to visit various other sites.

E. ^{129}Xe Chemical Shifts and the Size Effect. By using the approximate equations shown in section 2, we can obtain the ^{129}Xe chemical shift of various sizes of Xe_N clusters at different temperatures. The results of these calculations are shown in Figure 9. The calculated chemical shifts are close to the experimental values[2] for small Xe clusters at high temperatures. This may be due to the way we chose the parameter B. Our results, shown in Table 8, show the largest increases of the chemical shift at 300 K occurring between Xe_6 and Xe_7 and between Xe_7 and Xe_8. The increase is not as large as is found experimentally.[2] A plausible causative factor is the crowding of the Xe cluster inside the α cavities.[2] As the size of the Xe cluster increases, the contribution from Xe−Xe interaction becomes more important relative to the Xe−cavity interaction, especially in clusters with $N > 6$. Our equation for the chemical shift has a contribution from Xe−Xe interactions proportional only to R^{-6}. In the transition from Xe_6 to Xe_7, the Xe−Xe distance distribution might be expected to exhibit a significant change, particularly an increase in the relative contributions from short Xe−Xe distances. However in Figure 10, there are no obvious significant differences between the distance distributions of Xe_6 and Xe_7. The difference may be too subtle to be analyzed by such crude methods.

We now turn to the adsorption site model discussed previously, which already provided some insights regarding the crowding. On the basis of the number of adsorption sites and the distances between them, we expect that the cavity can accommodate 11 Xe atoms. Therefore, we naively might suspect that the crowding is due to the Xe−Xe interaction, not the Xe−cavity interaction. But from the energetic point of view, this cannot be the case. The Xe−cavity interaction is almost 10-fold larger than the Xe−Xe interaction. Even in a larger cluster, such as Xe_8, the total Xe−cavity interaction energy is

TABLE 5: Relative Site-Occupancy Times for Clusters of Two to Seven Xe Atoms inside the Cavity at Temperatures of 210, 300, and 420 K during a 1-ns Interval of a Typical Trajectory[a]

	site									
temp	0	1	2	3	4	5, 7, 10	6, 8, 9	11	12	13
					Xe_2					
210	6.3	22.7	34.1	2.5	3.8	18.8	8.1	0.6	2.5	6.8
300	11.9	25.9	17.2	7.1	8.6	8.2	15.1	2.7	2.4	6.8
420	17.5	13.7	14.0	8.4	8.6	13.6	15.6	3.4	2.2	2.5
					Xe_3					
210	4.5	25.3	24.8	3.0	4.4	13.1	21.0	1.0	2.2	0.4
300	10.7	20.3	15.3	10.1	11.4	9.7	14.4	2.8	2.5	2.3
420	16.8	14.9	15.9	8.3	7.3	13.4	13.6	3.4	3.1	2.9
					Xe_4					
210	5.1	19.9	20.4	10.6	12.6	14.3	12.0	3.2	1.2	0.4
300	9.4	16.9	14.1	8.5	9.8	14.2	17.5	3.3	2.7	3.3
420	14.1	12.0	14.3	9.0	8.1	15.5	14.9	3.3	4.3	4.0
					Xe_5					
210	3.59	19.2	18.1	9.8	7.5	17.6	17.3	1.6	2.9	2.1
300	8.6	15.0	16.4	9.1	9.1	14.3	15.2	3.3	4.3	4.5
420	13.4	13.6	12.5	8.0	7.8	14.1	17.0	3.0	4.9	5.5
					Xe_6					
210	4.0	16.0	15.7	9.6	6.8	16.3	16.9	2.7	8.3	3.4
300	7.0	15.2	14.5	8.0	8.3	16.4	16.0	4.2	6.2	5.6
420	10.4	13.6	13.7	7.7	8.1	15.8	15.6	2.7	5.7	6.8
					Xe_7					
210	4.4	14.0	14.0	9.4	9.0	16.4	17.1	3.4	5.8	6.2
300	6.6	13.4	13.3	9.1	9.1	16.1	16.1	4.0	5.4	6.0
420	10.0	12.6	11.8	8.2	8.5	16.2	16.4	4.2	6.2	5.6

[a] The column labeled site 0 is the percentage of time that none of the sites are occupied.

TABLE 6: Percentage of Desorption-and-Readsorption Events Resulting in Returning to the Same Site, for Clusters of Two to Seven Xe Atoms inside the Cavity at Temperatures of 210, 300, and 420 K during a 1-ns Segment of a Trajectory[a]

temp	0	1	2	3	4	5, 7, 10	6, 8, 9	11	12	13
					Xe_2					
210	53	67	81	38	36	18	0	0	0	25
300	37	61	58	18	23	18	28	11	0	0
420	28	54	51	19	21	15	16	0	0	11
					Xe_3					
210	48	71	67	33	28	38	8	0	0	0
300	38	73	61	26	34	15	27	7	5	4
420	32	56	60	23	19	24	31	13	2	2
					Xe_4					
210	40	82	78	18	29	34	30	5	0	0
300	31	63	64	18	23	28	21	4	2	10
420	28	56	56	26	21	19	18	7	12	14
					Xe_5					
210	36	94	88	7	8	52	41	5	16	11
300	33	76	82	22	15	28	24	5	21	16
420	37	64	67	25	23	46	34	5	16	17
					Xe_6					
210	40	97	94	17	17	44	51	8	24	22
300	39	90	87	14	14	38	38	2	24	22
420	38	87	85	22	28	31	31	3	18	17
					Xe_7					
210	39	100	100	24	19	29	51	13	15	23
300	40	98	92	33	25	53	50	11	13	17
420	40	91	89	29	23	43	46	8	24	19

[a] The column labeled site 0 is the average percentage of all events. Sites 5, 7, and 10 are treated as one site, and the same is true for sites 6, 8, and 9.

still larger than the total Xe−Xe interaction. How can the small contribution from Xe−Xe interactions outplay the much larger contribution due to the Xe−cavity interaction?

Two things are worth noting in Figure 11. First, the Xe−Xe average potential energy per atom reaches its minimum at Xe_7, but the total average potential energy per atom reaches a minimum at Xe_6. This is due to the less favorable Xe−cavity potential energy of Xe_7, as the figure shows. Secondly, in clusters smaller than Xe_7, the Xe−Xe potential decreases approximately 0.4 kJ/mol as the size of Xe clusters increases by one, but there is a sudden drop in this decrease between Xe_6 and Xe_7 and an increase in Xe−Xe potential energy between Xe_7 and Xe_8. That means that as a consequence of the growing relative contribution of the Xe−Xe interactions, the crowding

TABLE 7: Average Residence Time per Visit for Clusters of Two to Seven Xe Atoms inside the Cavity at Temperatures of 210, 300, and 420 K during a 1 ns Portion of a Trajectory[a]

	site									
temp	0	1	2	3	4	5, 7, 10	6, 8, 9	11	12	13
					Xe_2					
210	0.9	13.3	13.9	3.9	6.9	7.8	9.0	3.0	2.4	11.0
300	0.8	7.1	5.7	4.4	4.4	3.4	3.1	3.1	2.6	1.7
420	0.7	2.6	3.1	2.9	3.0	1.5	1.8	2.5	1.8	1.7
					Xe_3					
210	0.8	14.3	17.3	5.9	9.4	7.3	17.5	4.5	11.1	3.0
300	0.7	6.8	6.5	4.3	4.5	2.2	3.9	3.3	3.8	3.2
420	0.6	3.9	3.8	2.4	2.2	1.5	1.6	1.9	2.3	2.0
					Xe_4					
210	0.6	15.9	14.5	6.0	6.4	8.3	4.8	7.1	5.4	3.0
300	0.6	7.4	6.1	3.6	3.8	2.8	4.2	3.0	2.6	3.3
420	0.6	4.2	4.5	2.8	2.6	1.9	1.8	2.0	2.7	2.3
					Xe_5					
210	0.5	27.4	21.5	7.5	6.1	7.0	12.0	4.7	8.2	6.2
300	0.5	9.1	8.6	4.0	4.6	2.9	3.1	2.7	3.3	3.3
420	0.6	5.0	3.5	2.8	2.8	2.1	2.3	2.0	2.5	2.7
					Xe_6					
210	0.5	26.6	18.1	8.3	5.9	6.5	8.2	7.1	10.2	5.1
300	0.5	9.4	9.8	4.8	5.2	3.7	3.8	2.3	4.0	4.0
420	0.5	5.8	5.2	3.4	3.3	1.9	2.0	1.9	2.4	2.8
					Xe_7					
210	0.5	27.1	35.0	7.0	7.2	3.9	6.2	6.7	4.6	4.6
300	0.5	12.5	11.8	5.8	5.9	3.8	3.8	4.6	3.0	3.3
420	0.5	7.7	6.2	3.5	4.0	7.0	6.8	2.8	2.5	2.5

[a] The unit is picoseconds. The column labeled site 0 is the average residence time for Xe atoms in any site, between hops from site to site. The group of sites 5, 7, and 10 are treated as one site but normalized, i.e., divided by 3, and the same for sites 6, 8, and 9.

becomes important at Xe_7 and even more so at Xe_8. This can be explained by using the results found in the previous sections. According to the minimum-energy structures of Xe_7, the Xe atoms are forced to occupy sites near the other Xe atoms. The Xe cluster tries to balance between Xe−Xe and Xe−cavity interactions. This means that some Xe atoms occupy sites with large Xe−Xe repulsion but lower Xe−cavity attraction and cannot all fit into sites where that relation is reversed. (Note that the energy difference between sites 4 and 13 is just 3 kJ/mol.)

The precise meaning of "crowding" becomes this: with crowding, some Xe atoms are forced to occupy the energy-unfavorable sites or large Xe−Xe repulsion sites. This occurs first for clusters larger than Xe_6. Those Xe atoms in the energy-unfavorable sites are relatively mobile, so they are bound to collide with the other Xe atoms, but when they are in low-energy sites, they experience large Xe−Xe repulsion. The time history of the cluster, described in section 3.B, must include significantly more Xe−Xe collisions for clusters with $N > 6$ than for smaller clusters. The frequency of Xe−Xe collisions at small impact parameters is, we believe, the probable cause of the large changes in chemical shifts from $N = 6$ to $N = 7$ and then to $N = 8$. We expect there is an even larger increase in the chemical shift between Xe_8 and Xe_9. Figure 1 and an animation of Figure 8 are available on World Wide Web in the home directory http://rainbow.uchicago.edu/~fengli/cat.html.

4. Conclusion

In this paper, we have used an adsorption site model to clarify the roles of the Xe−Xe and Xe−wall interactions in the dynamics of Xe clusters inside zeolite cavities. Even though the Xe−wall interaction is much larger than Xe−Xe interaction, the energy differences between the adsorption sites are not much larger than the Xe−Xe repulsions. Atoms in smaller clusters, which have low-energy sites available for all of the Xe atoms, can move around without encountering the hindrance of large,

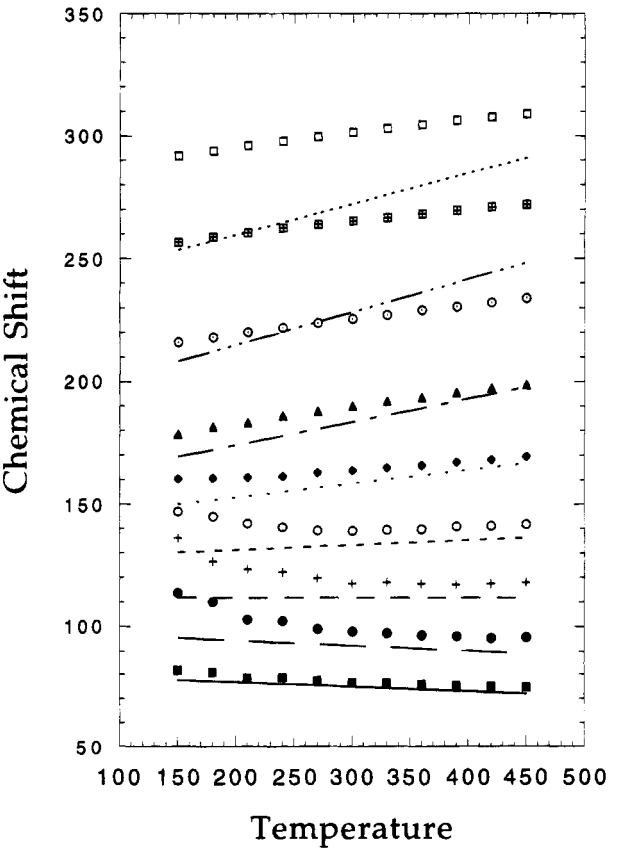

Figure 9. Chemical shifts of Xe_1 to Xe_9 averaged over a 10-ns trajectory. The unit of the X axis is ppm, and the unit of the Y axis is degrees Kelvin. The scatter points are calculated values, and the lines are generated from the slopes and the chemical shifts at 300 K, taken from experimental data of Table 8. The scatter points and the corresponding lines, in order from bottom to top, represent Xe_1 to Xe_9.

TABLE 8: Chemical Shifts of Xe_1 through Xe_8 at Temperature 300 K[a]

	n							
	1	2	3	4	5	6	7	8
				Experimental				
δ_n	74.8	92.3	111.7	133.2	158.4	183.5	228.3	272.3
$\delta_n - \delta_{n-1}$		17.5	19.4	21.5	25.2	25.1	45.1	43.7
$d\delta_n/dT$	−0.019	−0.020	0	0.020	0.056	0.095	0.133	0.125
				Calculated				
δ_n	76.6	97.9	117.4	140.1	163.9	190.0	225.7	265.3
$\delta_n - \delta_{n-1}$		21.3	19.5	22.7	23.8	26.1	35.7	39.6

[a] The experimental values and the slopes of chemical shift *vs* temperature are taken from ref 2.

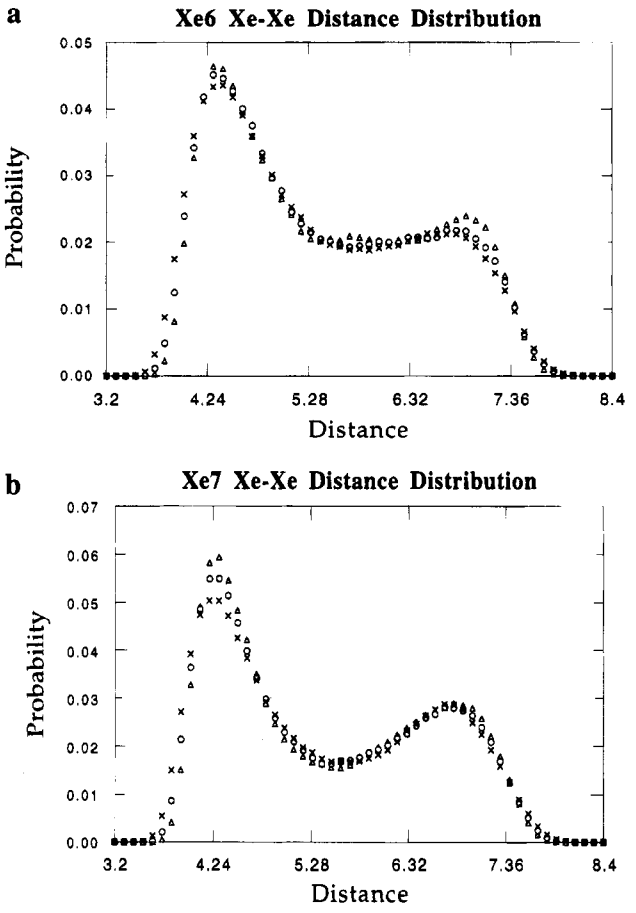

Figure 10. Xe−Xe distance distribution averaged over a 10-ns trajectory. The crosses represent data points taken at 420 K, the open circles, at 300 K, and the open triangles, at 210 K. The unit of length along the *X* axis is angstroms. The area under the curve is equal to 1. Part a is Xe_6, and part b is Xe_7.

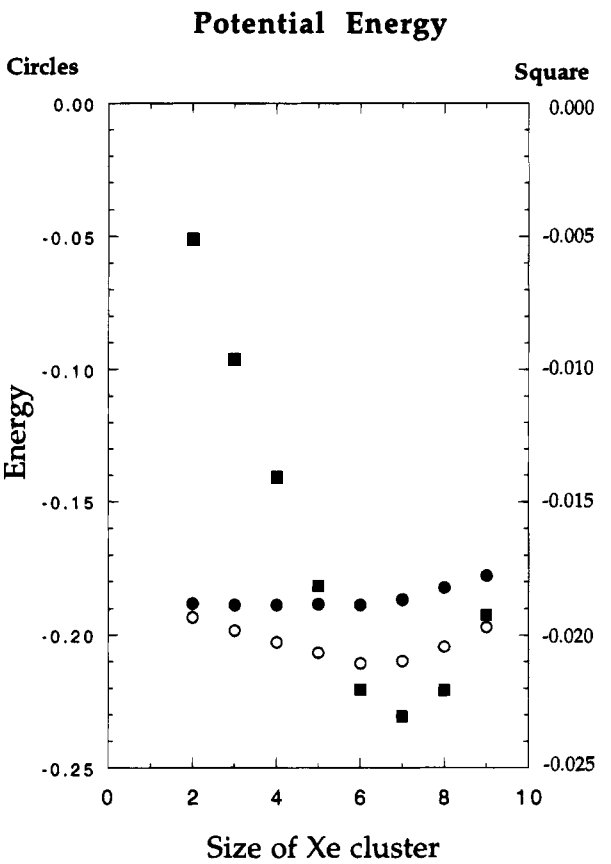

Figure 11. Potential energy averaged over a 10-ns trajectory. The filled circles represent the potential energy of the Xe−cavity interaction; the filled squares represent the potential energy of the Xe−Xe interaction; and the open circles represent the sum of the previous two energies. The *Y* axis has two different units. The one on the left is 10^5 J/mol for both the Xe−cavity interaction and total potential energy. The one on the right is 10^4 J/mol for the Xe−Xe interaction.

short-range Xe−Xe repulsive forces. But in larger clusters either congestion forces Xe atoms to occupy higher energy sites, which make them mobile, or some of the Xe atoms occupy the low-energy sites and experience large Xe−Xe nearest neighbor interactions. Both cases bring the Xe−Xe repulsive forces into play in the dynamics. This reveals itself in experiments, in particular, through the chemical shift. We attribute the large increase in chemical shift from Xe_6 to Xe_7 to this phenomenon. Nonetheless, even though the Xe−Xe interaction seems to play the dominant role in the dynamics of a cluster of xenon atoms inside the NaA zeolite α cavity, it is the balance of this interaction against the Xe−cavity interaction that governs the size and temperature dependence of the chemical shift.

As to the numerical values of the chemical shift, our computed results for Xe_N with $N < 7$ are satisfactory at temperatures above about 250 K but, except for the monomer, are too low at lower temperatures. For clusters of 7 and 8 atoms, our calculated chemical shifts show increases with temperature that are distinctly less than those found experimentally. We attribute the discrepancy for small clusters at low temperatures to our statistical algorithm, which starts each simulation in the lowest energy site. Especially at low temperatures, the finite sampling time gives the system very few opportunities to sample the phase space outside the well of its initial configuration. A more elaborate model would use as its initial condition a Boltzmann-weighted distribution of sites, rather than just the lowest energy sites. At temperatures above our lowest, there is enough mobility that the systems sample their phase space statistically within the time intervals that were practical for these simulations, so the results for all these other temperatures are not sensitive to the initial distribution.

The simple London expression we use for Xe−Xe chemical shift calculation must fail when the distance between Xe atoms is less than twice the van der Waals radius of the Xe atom. We

attribute our low values for the larger Xe clusters to this shortcoming of the model. A quantum version of the distance dependence of the chemical shift, such as the one used in ref 6, may be needed in these cases.

Finally, we changed the Xe−Xe interaction to the form suggested in ref 6. The result surprised us. Within a 1-ns interval of the trajectory of Xe_5 at 300 K, one of the Xe atoms escaped from the cavity, demonstrating that, with this potential function, a cavity network, and its boundary condition, the intercavity diffusion rate can be studied by simulation.

Acknowledgment. We would like to thank Dr. John P. Rose and Dr. Robert J. Hinde for helpful discussions, and Dr. Philip E. Rynes and Dr. Carl Dolnik for providing their graphics software. This research was supported by a grant from the National Science Foundation.

References and Notes

(1) Chemlka, B. F.; Raftery, D.; McCormick, A. V.; de Menorval, L. C.; Levine, R. D.; Pines, A. *Phys. Rev. Lett.* **1991**, *66*, 580.

(2) Jameson, C. J.; Jameson, A. K.; Gerald, R., III; de Dios; A. C. *J. Chem. Phys.* **1992**, *96*, 1676.

(3) Vernov, A. V.; Steele, W. A.; Abrams, L. *J. Phys. Chem.* **1993**, *97*, 7660.

(4) Loriso, A.; Bojan, M. J.; Vernov, A.; Steele, W. A. *J. Phys. Chem.* **1993**, *97*, 7665.

(5) Van Tassel, P. R.; Davis, H. T.; McCormick, A. V. *J. Chem. Phys.* **1993**, *98*, 8919.

(6) Jameson, C. J.; Jameson, A. K.; Baello, B. I.; Lim, H. M. *J. Chem. Phys.* **1994**, *100*, 5965, 5977.

(7) Wales, D. J.; Berry, R. S. *J. Chem. Phys.* **1990**, *92*, 4283.

(8) (a) Berry, R. S.; Beck, T. L.; Davis, H. L.; Jellinek, J. *Adv. Chem. Phys.* **1988**, *70*, 75. (b) Berry, R. S. In *The Chemical Physics of Atomic and Molecular Clusters*, Proceedings of the International School of Physics "Enrico Fermi", Course 107; Scoles, G., Ed.; North Holland: Amsterdam, 1990; pp 3−22. (c) Berry, R. S. In *The Chemical* Physics *of Atomic and Molecular Clusters*, Proceedings of the International School of Physics "Enrico Fermi", Course 107; Scoles, G., Ed.; North Holland: Amsterdam, 1990; pp 23−24.

(9) Cheng, H. P.; Berry, R. S. *Phys. Rev. A* **1992**, *46*, 791.

(10) Nosé, S. *J. Chem. Phys.* **1984**, *81*, 511.

(11) Yanagida, R. Y.; Amaro, A. A.; Seff, K. *J. Phys. Chem.* **1973**, *77*, 805.

(12) Van Tassel, P. R.; Davis, H. T.; McCormick, A. V. *Mol. Phys.* **1991**, *73*, 1107.

(13) Allen, M. P.; Tildesley, D. J. *Computer simulation of liquids*; Clarendon Press: Oxford, 1989; Chapter 3 and Appendix E.

(14) Jameson, A. K.; Jameson, C. J.; Gutowsky, H. S. *J. Chem. Phys.* **1973**, *53*, 2310.

JP941944B